tvst

Article

Straylight in Different Types of Intraocular Lenses

Augusto Arias[1], Harilaos Ginis[2], and Pablo Artal[3]

[1] Laboratorio de Óptica, Universidad de Murcia, Campus de Espinardo, Murcia, Spain
[2] Department of Research, Athens Eye Hospital, Glifada, Greece
[3] Laboratorio de Óptica, Universidad de Murcia, Campus de Espinardo, Murcia, Spain

Correspondence: Augusto Arias, Laboratorio de Óptica, CIOyN, Campus Espinardo (Ed.34), Murcia 30100, Spain. e-mail: augusto.arias@um.es

Received: May 14, 2020
Accepted: October 5, 2020
Published: November 9, 2020

Keywords: intraocular lens; cataract surgery; disability glare; optical quality; straylight

Citation: Arias A, Ginis H, Artal P. Straylight in different types of intraocular lenses. Trans Vis Sci Tech. 2020;9(12):16, https://doi.org/10.1167/tvst.9.12.16

Purpose: To show the importance of measuring the angular distribution of straylight as an in vitro test for intraocular lenses (IOLs).

Methods: The optical integration method was implemented to measure the point spread function, up to 5.1°, of IOLs immersed in a wet cell. The straylight parameter was calculated as the product of the point spread function by the squared angle. The effect of the scattered light is shown in extended images of a target surrounded by headlamps as glare sources. Three different IOLs were tested: (1) AcrySof IQ SN60WF, monofocal, (2) AcrySof IQ PanOptix, trifocal, and (3) Tecnis Symfony ZRX00, bifocal with extended depth of focus. Measurements were compared to previously reported clinical studies where the same IOL models were implanted.

Results: The mean amount of scattered light, between 1.0° and 5.1°, generated by each IOLs were, in $deg^2 sr^{-1}$ units: (1) 1.2, (2) 12.1, and (3) 33.4. Lens (3) present a high amount of straylight related to a halo of an approximate diameter of 2°.

Conclusions: In vitro measurements of the angular distribution of the point spread function of different types of IOLs showed important aspects related to their manufacturing quality. These results are in line with previous clinical findings where glare sensitivity was tested in the same angular range.

Translational Relevance: In vitro measurement of angular dependence of straylight in IOLs, regardless their design, provides a valuable feedback to improve their optical quality. The minimization of the amounts of straylight positively impacts the recurrence of photic phenomena.

Introduction

Since its invention, the implantation of intraocular lenses (IOLs) has significantly improved the quality of vision after cataract surgery. IOLs were initially designed with a single focus (monofocal) to restore far vision. Later, optics in the lenses became more sophisticated to provide intermediate and near vision by using segmented (multifocal) or continuous (extended depth of focus) focusing. These designs are based on refractive or diffractive approaches, or their combinations. A common approach to study the optical quality of IOLs is to record the point spread function (PSF). Typically, this is numerical and experimentally analyzed only in a narrow angular range, that is, less than 1°. The light distribution in the remaining angular range of the retina that is mainly affected by the scattered light or straylight, is associated to halos or the reduction of contrast sensitivity and may have a significant impact in the quality of vision of patients.

The in vitro evaluation of the angular distribution of straylight can provide useful information about the quality of IOLs beyond standard testing. Its implementation requires a proper methodology to measure the PSF over a wide angular range. The direct acquisition of the PSF with a two-dimensional array of detectors (e.g., CCD or CMOS cameras) is suitable to partially assess the optical quality of the IOL but not for the straylight measurement because of the limited dynamic range (typically 8 bits) of the sensors. Therefore, one alternative is to change the gain or exposure time to enhance the digitalized signal once the device is mounted in a goniometer to scan the light distribution at large angles while the IOL is illuminated by a collimated beam.[1] Other proposed option was the

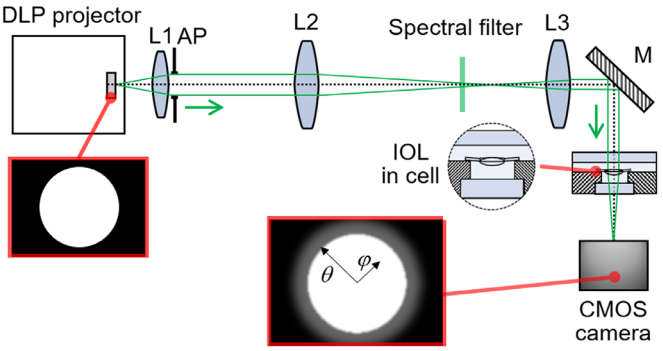

Figure 1. Experimental setup for the reconstruction of the PSF and straylight. DLP, digital light projector.

adaptation of a C-Quant device (Oculus Optikgeräte GmbH, Wetzlar, Germany) to psychophysically estimate the mean amount of straylight, over a certain angular range, from monofocal and multifocal IOLs in wet cells.[2,3]

In this work, the optical integration method was implemented to objectively retrieve the angular distribution of the PSF in a large visual field. This methodology, that does not require moving parts or specialized detectors, has been previously employed for both the in vitro[4,5] and in vivo[6–8] estimation of the angular profile of intraocular straylight.

Three IOLs with different designs were tested and were compared with the expected optical response for a standard observer according to the International Commission on Illumination (CIE [*Commission Internationale de l'Eclairage*]).[9] Moreover, the veil of luminance caused by the scattered light from each IOL was quantified in conditions resembling a real-world visual scene with the presence of glare sources. These findings were compared with previously reported clinical observations with the same tested IOLs models.

Methods

Optical Integration Method

The instrument is schematically represented in Figure 1. It is based on the optical integration method where uniform disks with varying radius, generated with a Digital Light Projector (DLP, LightCrafter Display 4710 EVM; Texas Instruments Inc., Dallas, TX), are imaged through the IOL under test. The L1 lens collimated the beam from the projector. A telescope with magnification of 0.5 conjugates the circular aperture AP, in front of the L1 lens, and the IOL which is inside a cell filled with physiological saline (0.9% NaCl) solution. A spectral filter (FB550-40; Thorlabs Inc., Bergkirchen, Germany) was incorporated into the telescope to provide a quasimonochromatic illumination with a central wavelength and bandwidth of 550.4 and 42.0 nm, respectively. The images of the disks formed by the system were recorded by a CMOS camera (DCC1545M; Thorlabs Inc.) placed at the focal plane of the IOL. The axial displacement of the camera allows to select different foci in the case of multifocal IOLs. As a reference, a biconvex lens (LB1450; Thorlabs Inc.) was also measured to estimate the baseline of straylight generated by the optical components of the instrument.

The central intensity of the recorded disks is the sum of all contributions from every bright point in the projected disk. Such contribution is proportional to the PSF valued at a given φ angle. Thus, the central intensity can be mathematically expressed as:

$$I_c(\theta) = \int_0^{\theta} 2\pi\varphi PSF(\varphi)\, d\varphi \tag{1}$$

where θ is the visual angle. Then, as a consequence of Eq. (1), the PSF can be calculated as the angular derivative of the central intensity:

$$PSF(\theta) = \frac{1}{2\pi\theta}\frac{dI_c(\theta)}{d\theta} \tag{2}$$

This equation is numerically solved by calculating the local slopes of the central intensity. Then, the scattered light, or straylight, is quantified through the straylight parameter s which is calculated as[10]:

$$s(\theta) = \theta^2 PSF(\theta) \tag{3}$$

The central intensity was measured by integrating the digitalized intensity over an area of 0.03 × 0.03 deg^2 while the disks were projected. The radius of those disks was gradually increased with three angular resolutions (in degrees): 0.027 for radii lower than 1.34, 0.068 for radii between 1.41 and 3.38, and 0.135 for radii larger than 3.51. The background was removed from the data. In each series of measurements, the central intensity, as function of the angular radius of the disk, was estimated three times and averaged. Residual high-frequency fluctuations were removed by applying a low-pass filter. The local slopes of the central intensities were calculated by linear fitting the data within windows with a width of nine elements along the angular range.

The angles of the PSFs are mainly constrained by the focal length of lenses L1, L2, and L3 and the resolution of the Digital Light Projector. The lower limit is larger than the subtended angle by one digital light projector's pixel to draw well-shaped disks, fulfilling this implicit condition in Eq. (1). Thus, the lower angle is 0.12°, that is, only disks with a radius larger or equal

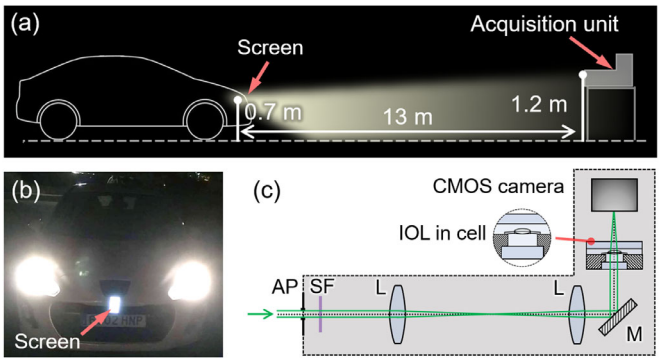

Figure 2. **(a)** Sketch of the outdoor experiment to register the effect of the headlamps as glare sources on imaging. **(b)** Location of the smartphone between the headlamps. **(c)** Acquisition unit where the IOL is conjugated with a circular aperture (AP). The spectral filter (SF) blocks the infrared light.

to 9 pixels were projected. The upper limit is 5.1° and, therefore, the retrieved PSFs are normalized to this value. Despite this, measurements can be compared with the empirical formulations of the ocular PSF provided by the CIE (CIE PSF) that are normalized up to 90°. For an accurate comparison, the latter were renormalized up to 5.1° by a coefficient calculated as the ratio between the areas under the CIE PSF up to that angle and 90°.

Imaging a Scene with Glare Sources through the IOL

The effects of scattered light is better visualized when glare sources (e.g., the headlamps of a car) are present in a scene. Figure 2 shows the experimental setup arranged to register the veiling glare from a pair of headlamps. A screen of a smartphone was placed between the headlamps, serving as a reference. The headlamps (dipped beam) were halogen and correspond to the series equipment of a small family car (Peugeot 308, 2012 model). The screen was displaying a white background with a luminance of 363 cd/m^2. The full scene was registered by an acquisition unit composed of a telescope with unitary magnification that conjugates a circular aperture with a diameter of 4 mm and the IOL. The images at the far focus of each IOL were acquired by an CMOS camera (BFS-U3-120S4M-CS; FLIR Systems Inc., Wilsonville, OR). A spectral filter (FES0650; Thorlabs Inc.) was incorporated into the telescope to reject the infrared light where the camera was still sensitive but is not the eye. The gamma value of the camera was set on 0.45 as a primary tone mapping operator.

Light intensity in the acquired images was estimated, in arbitrary units, after a calibration of the camera in the acquisition unit. This calibration consists of assigning luminance values to the digitalized intensity values by using a luminance meter (LS-100; Konica-Minolta Inc., Tokyo, Japan) while both devices are imaging a screen with different programmed gray levels. Thus, the light intensity is proportional to the measured luminance. A background image associated to the dark current of the camera at the specific settings was also subtracted from all acquired images.

Tested IOLs

Three unused IOLs were tested: AcrySof IQ SN60WF (Alcon Laboratories Inc., Forth Worth, TX), monofocal; AcrySof IQ PanOptix TFNT00 (Alcon Laboratories Inc.), trifocal; and Symfony ZXR00 (Abbott Medical Optics Inc., Nieuwegein, the Netherlands), bifocal with extended depth of focus. Their main characteristics are summarized in the Table. The narrow-angle PSF and the modulation transfer function of these IOLs have been already evaluated in vitro.[11–13] In addition, their impact on the quality of vision has been clinically studied through the visual acuity and contrast sensitivity, as well as the incidence rate of photic phenomena (e.g., halos, flashes, starbursts, and glare).[14–16] The three IOLs were taken from random batches.

Results

Figure 3a shows the normalized central intensities of the recorded disks as function of their radius for each IOL and the reference lens (as baseline) in their main focal planes. PSFs (Fig. 3b) were obtained by applying Eq. (2) to the central intensities and compared with the CIE function for a 70-year-old observer (dashed black line).

Results for both the baseline and the monofocal (SN60WF) IOL are similar. As the angular range of the retrieved PSF is from 0.12° to 5.10°, the effect of the asphericity in the monofocal IOL is not appreciated because it occurs at narrower angles. Likewise, for the multifocal or extended depth of focus IOLs, the PSF profiles at different focal planes were similar, being slightly different in the case of the PanOptix for the near focus with respect to the other two profiles. Figure 4 shows the calculated angular dependence of straylight for the baseline and the IOLs at the focal plane for far vision. The mean of the induced amounts of straylight (i.e., values subtracted by the baseline) between 1.0° and 5.1° for each IOL are (in deg^{2}sr^{-1} units): SN60WF, 1.2; PanOptix, 12.1; and Symfony, 33.4.

Table. Characteristics of the Tested IOLs

IOL Model	AcrySof IQ SN60WF	AcrySof IQ PanOptix TFNT00	Symfony ZXR00
Design	Aspheric	Aspheric, diffractive	Aspheric, diffractive
Nominal power (diopters)	20	22.5, +2.0 and +3.2	22.50 and +1.75[11]
Diameter of diffractive zone	–	4.5 mm[14]	4.9 mm[14]
Material	Hydrophobic acrylate	Hydrophobic acrylate/ methacrylate copolymer	Hydrophobic acrylate

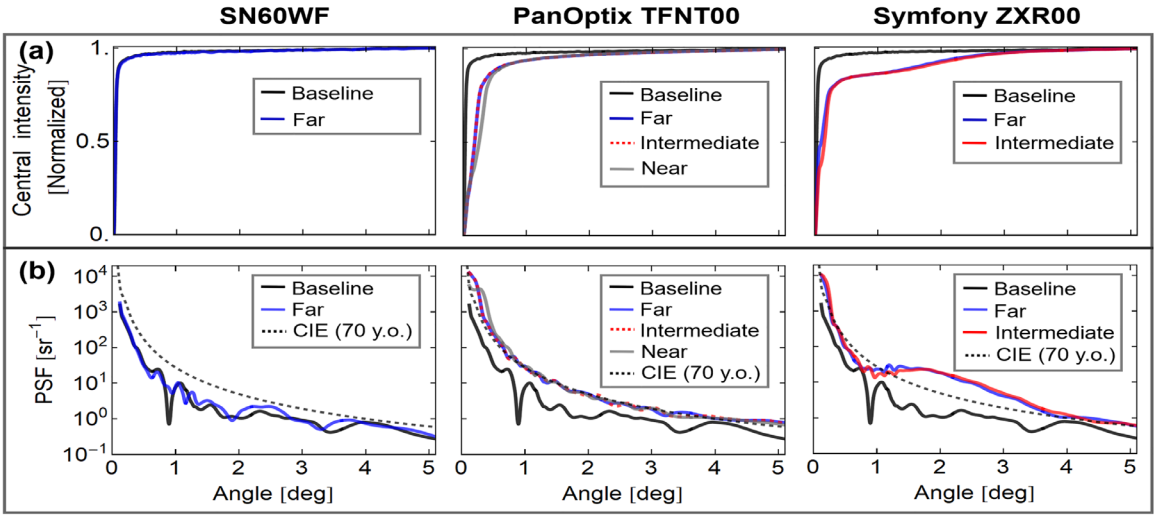

Figure 3. **(a)** Central intensity and **(b)** PSF as function of the angle for the baseline and tested IOLs at their focal planes.

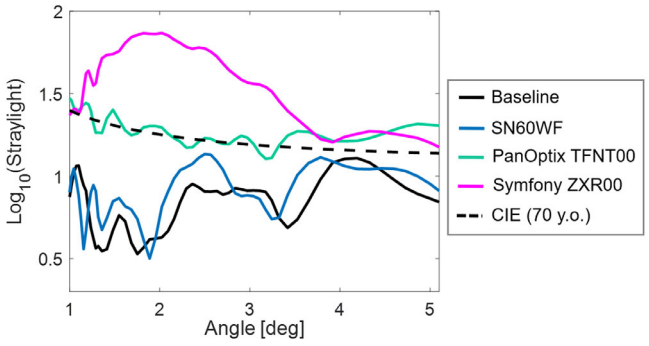

Figure 4. Angular dependence of straylight for the baseline, the tested IOLs and a 70-year-old standard observer.

Figure 5 shows the recorded images of the head lamps and a smartphone screen acquired through the different tested IOLs. The ratio between the intensities of the scattered light around the headlamps, between 1.0° and 2.2°, and the smartphone screen—through the monofocal IOL—for each IOL is (mean, maximum): SN60WF, 0.03, 0.19; PanOptix, 0.08, 0.32; and Symfony, 0.14, 0.76.

Discussion

The angular dependence of the PSF and the straylight parameter were estimated in vitro for three different types of IOLs. According to the comparison of the normalized PSF profiles (Fig. 3b), the optical quality of the SN60WF (monofocal) IOL does not differ from that for a lens manufactured for scientific applications (i.e., the baseline). However, higher values of straylight were found in both the PanOptix and Symfony IOLs regardless the selected focal plane. The measured values of intraocular straylight

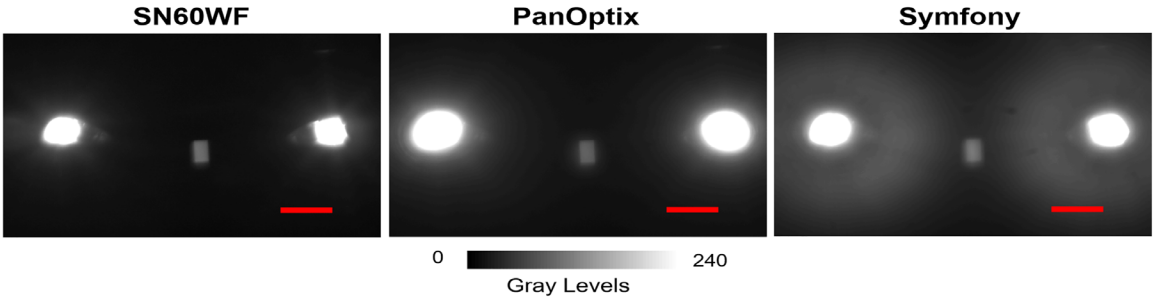

Figure 5. Acquired images of the scene shown in Figure 2 through the tested IOLs. Length of *red bars* is 1°.

in these IOLs are similar or higher than those found in a 70-year-old standard observer. The values are notably higher for the Symfony IOL between 1° and 4° with a peak maximum located at 1.82°. This result may be produced by variations in the refractive index and/or surface height with a period around 17 microns. Specular microscopy images[11] shown nonhomogeneous microrings within the diffractive etching of the Symfony IOL that presumably generate this elevated amounts of scattered light. We inspected the tested IOLs, confirming the presence of those microrings in the Symfony IOL. This kind of structures, previously studied in multifocal IOLs,[17] could be produced by diamond lathing of the diffractive pattern. Beyond the quantification of the scattered light, it was also visualized in a scene with car headlamps (Fig. 5). The intensity of the scattered light around the headlamps follows the corresponding angular values of each IOL's PSF.

Some clinical measurements of straylight and its effects in eyes implanted with the same IOL models tested here[18,19] are not in full agreement with our findings. However, it is necessary to take into account that straylight is commonly reported as a single value that corresponds with the average over a defined angular range. Because those ranges may vary among the different instruments, the experimental and clinical measurements have to be carefully compared and discussed. For example, Monaco et al.[18] measured the following average scattering amounts (in logarithmic units) in 40 bilaterally implanted eyes with each IOL model by using a C-Quant device: SN60WF, 0.82 ± 0.22; PanOptix, 0.87 ± 0.20; and Symfony, 0.86 ± 0.21. Thus, low mean amounts of straylight were found from 5° up to 10°, with no significant differences among the three IOL models. Indeed, this is complementary but not contradictory to our results that account for values of straylight determined between 1.0° and 5.1°. Similarly, Pilger et al.[19] did not find differences in the glare sensitivity of patients implanted with the Symfony and Tecnis ZCB00 (monofocal; Abbott Medical Optics Inc.) IOLs. Although we did not evaluate the latter, one would expect lower amounts of straylight in the monofocal IOL because of its possible polishing. They used a Mesoptometer II (Oculus Optikgeräte GmbH) device to assess the mesopic contrast sensitivity with and without glare. In that instrument, the glare consists of a luminous point placed 3° away from the stimulus.[20] According to our measurements, the straylight values at 3° of the Symfony IOL are higher than the baseline (or the monofocal SN60WF) but not the highest, as shown in Figure 4. Indeed, for this particular IOL, Figure 5 shows than the luminance of the scattered light from a headlamp drastically decreases for angles larger than 2° approximately. Therefore, the veil could not be sufficiently luminous to lead a contrast reduction at 3°. In contrast, de Medeiros et al.[21] have shown a lower glare disability in a group of patients with bilateral implantation of the PanOptix IOLs than in another group with blended implantation of the Symfony and Tecnis ZMB00 (bifocal; Abbott Medical Optics Inc.) IOLs. They used a CSV-1000 chart where the lamps that act as glare sources are next to the stimulus. The contrast sensitivity values in the Symfony/ZMB00 group were decreased throughout all spatial frequencies after the glare was turned on, being a representative effect of the straylight.[22] It is important to point out that microrings were observed in the ZMB00 model[11] which presumably would increase the amount of straylight, as in the Symfony. Escandón-García et al.[23] indirectly quantified the glare disability using an instrument with an angular range up to 2.7°,[24] which agrees with our experimental conditions. The participants of that study were bilaterally implanted with the PanOptix, Symfony and other multifocal IOL. The glare effects were higher in the patients treated with Symfony, being in line with our results.

Additionally, some of the clinical studies discussed in this article also evaluated the recurrence of photic

phenomena in the treated patients through surveys. In the study of Monaco et al.,[18] the percentage of the participants who rated "never" to the glare symptoms was significant larger in the case of SNFW60 than for PanOptix and Symfony IOLs, as expected, but it was slightly higher for the Symfony than the PanOptix. Pilger et al.[19] report higher rates of glare in patients implanted with Symfony than the monofocal Tecnis ZCB00. Similar conclusions were published by the Symfony's manufacturer.[25] Although the size of our sample does not justify a generalization about the possible performance of large series of lenses or different production batches, those clinical findings are in line with our experimental results. However, the effect of the neural adaptation must be taken into account to entirely understand the tolerance of implanted patients to photic phenomena. Our results were fully based in optical measurements, which allow for a fair comparison among different lenses directly.

In conclusion, the in vitro reconstruction of the PSF (up to 5.1°) and the estimation of the straylight parameter of IOLs provides relevant information concerning the quality of their manufacturing process and can explain clinical measurements where those quantities are commonly simplified with single value metrics. Although the monofocal IOL tested showed minimal scattered light, we particularly found a large amount of scattered light, in a range between 1° and 4° of visual angle, in the Symfony IOL. Such amount of scatter could affect the quality of vision of a implanted patient. Further studies are required to determine if the presented findings correspond with the generalized performance of the IOL models, because our sample is not representative. The optical integration method can be a useful methodology for further studies to evaluate IOLs with different materials and the glistening formation.

Acknowledgments

Supported by European Research Council (ERC-2013-AdG-339228); Secretaría de Estado de Investigación, Desarrollo e Innovación (FIS2016-76163-R); Fundación Séneca (19897/GERM/15); European Regional Development Fund (EU-FEDER); and The Operational Program Competitiveness, Entrepreneurship and Innovation, under the call RESEARCH - CREATE - INNOVATE (project code: T1EDK03913).

Disclosure: **A. Arias,** None; **H. Ginis,** P, C; **P. Artal,** P, F

References

1. Langeslag MJM, van der Mooren M, Beiko GHH, Piers PA. Impact of intraocular lens material and design on light scatter: in vitro study. *J Cataract Refract Surg*. 2014;40(12):2120–2127, doi:10.1016/j.jcrs.2014.10.017.
2. Łabuz G, Reus NJ, van den Berg TJTP. Straylight from glistenings in intraocular lenses: in vitro study. *J Cataract Refract Surg*. 2017;43(1):102–108, doi:10.1016/j.jcrs.2016.10.027.
3. Łabuz G, Vargas-Martín F, van den Berg TJTP, López-Gil N. Method for in vitro assessment of straylight from intraocular lenses. *Biomed Opt Express*. 2015;6(11):4457, doi:10.1364/boe.6.004457.
4. Ginis H, Pentari I, de Brouwere D, Bouzoukis D, Naoumidi I, Pallikaris I. Narrow angle light scatter in rabbit corneas after excimer laser surface ablation. *Ophthalmic Physiol Opt*. 2009;29(3):357–362, doi:10.1111/j.1475-1313.2009.00649.x.
5. Arias A, Ginis H, Artal P. Light scattering in the human eye modelled as random phase perturbations. *Biomed Opt Express*. 2018;9(6):2664, doi:10.1364/BOE.9.002664.
6. Ginis H, Perez GM, Bueno JM, Artal P. The wide-angle point spread function of the human eye reconstructed by a new optical method. *J Vision*. 2012;12(3):20–20, doi:10.1167/12.3.20.
7. Ginis HS, Perez GM, Bueno JM, Pennos A, Artal P. Wavelength dependence of the ocular straylight. *Investig Ophthalmol Vis Sci*. 2013;54(5):3702, doi:10.1167/iovs.13-11697.
8. Christaras D, Ginis H, Pennos A, Artal P. Intraocular scattering compensation in retinal imaging. *Biomed Opt Express*. 2016;7(10):3996–4006, doi:10.1364/BOE.7.003996.
9. Vos JJ, Cole BL, Bodmann H-W, Colombo E, Takeuchi T, van den Berg TJTP. CIE equations for disability glare. 2002.
10. van den Berg TJ. Analysis of intraocular straylight, especially in relation to age. *Optom Vis Sci*. 1995;72(2):52–59, doi:10.1097/00006324-199502000-00003.
11. Gatinel D, Loicq J. Clinically relevant optical properties of bifocal, trifocal, and extended depth of focus intraocular lenses. *J Refract Surg*. 2016;32(4):273–280, doi:10.3928/1081597X-20160121-07.
12. Carson D, Xu Z, Alexander E, Choi M, Zhao Z, Hong X. Optical bench performance of 3 trifocal intraocular lenses. *J Cataract Refract Surg*. 2016;42(9):1361–1367, doi:10.1016/j.jcrs.2016.06.036.

13. Loicq J, Willet N, Gatinel D. Topography and longitudinal chromatic aberration characterizations of refractive–diffractive multifocal intraocular lenses. *J Cataract Refract Surg*. 2019;45(11):1650–1659, doi:10.1016/j.jcrs.2019.06.002.
14. Sudhir RR, Dey A, Bhattacharrya S, Bahulayan A. Acrysof IQ panoptix intraocular lens versus extended depth of focus intraocular lens and trifocal intraocular lens: a clinical overview. *Asia Pac J Ophthalmol (Phila)*. 2019;8(4):335–349, doi:10.1097/APO.0000000000000253.
15. Liu J, Dong Y, Wang Y. Efficacy and safety of extended depth of focus intraocular lenses in cataract surgery: a systematic review and meta-analysis. *BMC Ophthalmol*. 2019;19(1):198, doi:10.1186/s12886-019-1204-0.
16. Breyer DRH, Kaymak H, Ax T, Kretz FTA, Auffarth GU, Hagen PR. Multifocal intraocular lenses and extended depth of focus intraocular lenses. *Asia Pac J Ophthalmol (Phila)*. 2017;6(4):339–349, doi:10.22608/APO.2017186.
17. Wenzel MR, Imkamp EM, Apple DJ. Variations in manufacturing quality of diffractive multifocal lenses. *J Cataract Refract Surg*. 1992;18(2):153–156, doi:10.1016/S0886-3350(13)80922-4.
18. Monaco G, Gari M, di Censo F, Poscia A, Ruggi G, Scialdone A. Visual performance after bilateral implantation of 2 new presbyopia-correcting intraocular lenses: trifocal versus extended range of vision. *J Cataract Refract Surg*. 2017;43(6):737–747, doi:10.1016/j.jcrs.2017.03.037.
19. Pilger D, Homburg D, Brockmann T, Torun N, Bertelmann E, von Sonnleithner C. Clinical outcome and higher order aberrations after bilateral implantation of an extended depth of focus intraocular lens. *Eur J Ophthalmol*. 2018;28(4):425–432, doi:10.1177/1120672118766809.
20. Schlote T, Kriegerowski M, Bende T, Derse M, Thiel HJ, Jean B. Mesopic vision in myopia corrected by photorefractive keratectomy, soft contact lenses, and spectacles. *J Cataract Refract Surg*. 1997;23(5 Suppl.):718–725, doi:10.1016/S0886-3350(97)80280-5.
21. de Medeiros AL, de Araújo Rolim AG, Motta AFP, et al. Comparison of visual outcomes after bilateral implantation of a diffractive trifocal intraocular lens and blended implantation of an extended depth of focus intraocular lens with a diffractive bifocal intraocular lens. *Clin Ophthalmol*. 2017;11:1911–1916, doi:10.2147/OPTH.S145945.
22. van den Berg TJTP, Franssen L, Coppens JE. Ocular media clarity and straylight. In: *Encyclopedia of the Eye*. New York: Elsevier/Academic Press; 2010:173–183, https://pure.knaw.nl/portal/en/publications/ocular-media-clarity-and-straylight(0588466a-fd51-4bb9-90d4-f1169b1108a6)/export.html. Accessed July 17, 2018.
23. Escandón-García S, Ribeiro FJ, McAlinden C, Queirós A, González-Méijome JM. Through-focus vision performance and light disturbances of 3 new intraocular lenses for presbyopia correction. *J Ophthalmol*. 2018;2018, doi:10.1155/2018/6165493.
24. Linhares JMM, Neves H, Lopes-Ferreira D, Faria-Ribeiro M, Peixoto-De-Matos SC, Gonzalez-Meijome JM. Radiometric characterization of a novel LED array system for visual assessment. *J Mod Opt*. 2013;60(14):1136–1144, doi:10.1080/09500340.2013.842614.
25. Abbott Medical Optics, Inc. Patient information brochure, https://www.accessdata.fda.gov/cdrh_docs/pdf/P980040S065C.pdf. Accessed February 1, 2020.